



Effects of Al and N plasma immersion ion implantation on surface microhardness, oxidation resistance and antibacterial characteristics of Cu

Quan-zhang AN^{1,2,3}, Kai FENG¹, He-ping LÜ¹, Xun CAI¹, Tie-tun SUN³, Paul K. CHU²

1. Shanghai Key Laboratory of Materials Laser Processing and Modification,

School of Materials Science and Engineering, Shanghai Jiao Tong University, Shanghai 200240, China;

2. Department of Physics and Materials Science, City University of Hong Kong, Hong Kong 999077, China;

3. Changzhou EGing Photovoltaic Technology Co., Ltd., Changzhou 213200, China

Received 20 June 2014; accepted 4 November 2014

Abstract: Al and N were introduced into copper substrate using plasma immersion ion implantation (PIII) in order to enhance its hardness and oxidation resistance. The dosage of N ion is $5 \times 10^{16} \text{ cm}^{-2}$, and range of dosage of Al ion is $5 \times 10^{16} - 2 \times 10^{17} \text{ cm}^{-2}$. The oxidation tests indicate that the copper samples after undergoing PIII possess higher oxidation resistance. The degree of oxidation resistance is found to vary with implantation dosage of Al ion. The antibacterial tests also reveal that the plasma implanted copper specimens have excellent antibacterial resistance against *Staphylococcus aureus*, which are similar to pure copper.

Key words: copper; plasma immersion ion implantation; nanoindentation; oxidation resistance; antibacterial properties

1 Introduction

Besides the application in microelectronic packaging [1], copper has been used as an excellent antibacterial agent for many years [2–4], for its high bactericidal rate to many bacteria such as *Staphylococcus aureus* [5] and *Escherichia coli* [6,7]. Compared with organic antibacterial agents, metal copper has desirable properties such as good machinability, stability, relative non-toxicity, and broad spectrum antibiotics boasting high antibacterial activity against both bacteria and fungi. However, copper still has suffered some disadvantages such as low hardness compared with other metals such as stainless steels and vulnerable to oxidation, thereby limiting its applications. It is known that the surface performances of copper can affect its antibacterial properties as well as appearance. Therefore, it is significant to improve the surface hardness and enhance the oxidation resistance of copper while not compromising its other desirable properties.

The mechanical properties of copper can be improved by electrodeposition [8–10] and its oxidation resistance has been enhanced by means of electroless

deposition [11], chemical vapor deposition [12], and other methods [13,14]. Among the surface modification techniques, ion implantation is an effective method to modify the mechanical and chemical properties such as hardness, wear, fatigue, friction, and oxidation resistance, of metal and non-metal materials [15–17]. The improved mechanical properties can usually be attributed to radiation-enhanced diffusion, ion-induced chemical reactions, grain refinement, and defect generation. Recently, plasma immersion ion implantation (PIII) has attracted much attention as this technique offers unique advantages including the possibility to treat large industrial components with complex shape without extensive sample manipulation as well as high dose rate and large area capabilities [18]. Up to now, most of the existing literature about Cu ion implantation has focused on materials modified by Cu ion implantation [19–21], but the literature on enhancing properties of copper by ion implantation is seldom [22].

In this work, copper samples were implanted sequentially with aluminum and nitrogen at lower negative bias and different Al implantation dosages. Our results disclose that the implanted copper specimens have not only higher hardness, but also better oxidation

resistance. The PIII-treated copper samples show good antibacterial performance: they have an almost 100% bactericidal rate against *Staphylococcus aureus*, which is similar to that observed on pure copper. The lower negative bias employed in the PIII process and low cost enable commercialization of the experimental protocols described in this work.

2 Experimental

2.1 Sample preparation

Copper samples were mechanically polished and cleaned before undergoing PIII. Al and N were implanted into the copper samples successively using a PIII instrument equipped with Al cathodic arc source and nitrogen gas plasma sustained by radio frequency (RF) excitation. The detailed preparation procedures can be found in Ref. [23]. In this work, Samples S1, S2, S3, S4, S5 and S6 were subjected to different treatments and the treatment parameters are summarized in Table 1.

Table 1 Main processing and instrumental conditions

Sample	Process condition
S1	Pure copper control (untreated)
S2	PIII: Sample bias -30 kV, Al implant dosage $5 \times 10^{16} \text{ cm}^{-2}$, N implant dosage $5 \times 10^{16} \text{ cm}^{-2}$
S3	PIII: Sample bias -30 kV, Al implant dosage $2 \times 10^{17} \text{ cm}^{-2}$, N implant dosage $5 \times 10^{16} \text{ cm}^{-2}$
S4	S1 after oxidation*
S5	S2 after oxidation*
S6	S3 after oxidation*

*Parameters of oxidation process in Ref. [23]: 1) Heating from room temperature to 260°C at rate of $20^\circ\text{C}/\text{min}$; 2) Maintained at 260°C for 1 h; 3) Cooled down to room temperature naturally

2.2 Characterization of mechanical properties and oxidation resistance

The mechanical properties of Samples S1, S2 and S3 were determined using continuous stiffness measurements by nanoindentation on the MTS Nano Indenter (XP) system. The nanoindentation tests were conducted in air at room temperature, and each sample was measured three times at different locations to obtain the corresponding mean values. X-ray photoelectron spectroscopy (XPS, physical electronics PHI–5802) was employed to determine the depth profiles and valence states of oxygen and copper in Samples S4, S5 and S6. A sputtering rate of $25.9 \text{ nm}/\text{min}$ was used for Sample S4 and a sputtering rate of $1.84 \text{ nm}/\text{min}$ was used for Samples S5 and S6.

2.3 Antibacterial activities

Staphylococcus aureus ATCC6538 (*S. aureus*, Gram-positive) was used to evaluate the antibacterial properties of Samples S1, S2 and S3 by the plate-counting method in which pure copper was used as the positive control and the culture dish was used as the negative control. To guarantee the accuracy of measuring values, each group contains three parallel samples. Before the antibacterial test, the samples were sterilized with 75% ethanol overnight and air dried. Then, 0.1 mL solution of bacteria (2×10^5 – $5 \times 10^5 \text{ CFU}/\text{mL}$) was added onto the surface of each sample and covered by a polyethylene (PE) film ($15 \text{ mm} \times 15 \text{ mm}$). The bacteria were subsequently added onto the samples which were incubated at 37°C and about 90% humidity for 24 h. Afterwards, they were thoroughly washed with a sterile phosphate-buffered saline (PBS) solution that contained 0.1% Tween 80 with pH 7.2–7.4. To observe the living bacteria, 1, 0.1 and 0.01 mL of the washing solutions were added to different dishes containing the nutrient agar. After 24 h of incubation under similar conditions, the subsequent macroscopic bacterial colonies were counted and the antibacterial effect was quantitatively determined using the following equation [24]:

$$R = \frac{B - C}{B} \times 100\% \quad (1)$$

where R , B and C are the antibacterial effect, the mean number of bacteria on the control samples (CFU/sample), and the mean number of bacteria on the modified samples, respectively.

3 Results and discussion

3.1 Mechanical properties

Figure 1 depicts the load versus depth curves and hardness versus depth curves of Samples S1, S2 and S3. It can be seen from Fig. 1(a) that a higher load is needed to penetrate the same depth for Samples S2 and S3 compared with Sample S1, and so the plasma implanted samples have higher hardness as shown in Fig. 1(b). The higher hardness of Samples S2 and S3 may be attributed to lattice distortion resulting from irradiation damage and defects including cavities and interstitial atoms. It can be seen from Fig. 1(b) that the maximum hardness of Sample S3 at the depth of 7–8 nm is about 3 times that of Sample S1, whereas the maximum hardness of Sample S2 is about twice that of Sample S1. One possible explanation is that the larger Al implantation dosages result in higher radiation damage and more defects.

3.2 Oxidation behavior

Figure 2 displays the changes in the oxidation

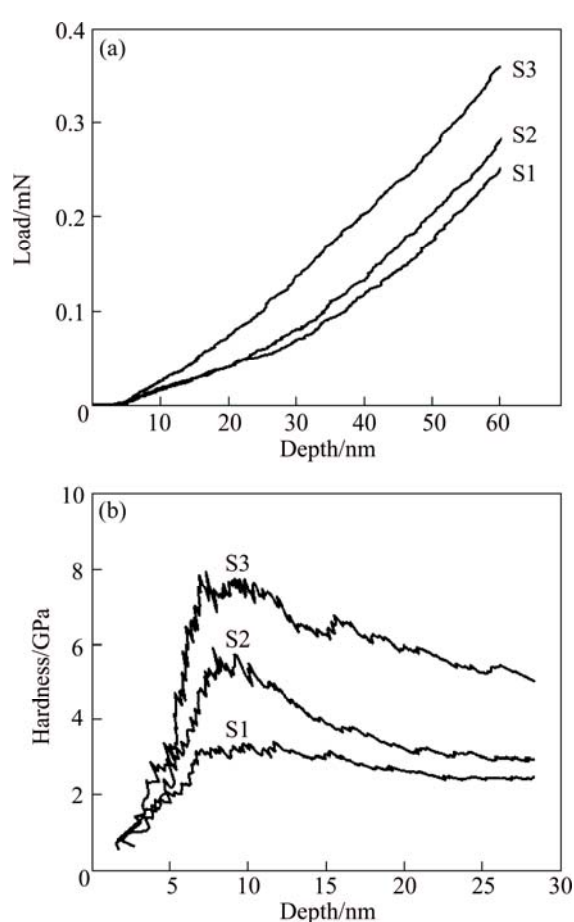


Fig. 1 Surface mechanical proprieties of Samples S1, S2 and S3: (a) Load vs indentation depth curves; (b) Hardness vs indentation depth curves

behavior of the implanted samples after being exposed to air at 260 °C for 1 h. Comparing the elemental distributions of Samples S5 and S6 with that of Sample S4, the penetration of oxygen in Samples S5 and S6 is much smaller. In Sample S4, oxygen extends to a depth of 240–275 nm. In comparison, in Samples S5 and S6, oxygen can only be found up to depths of 45 and 35 nm, respectively. The oxygen depth in Sample S6 is only about 1/9 of that in Sample S4, and the maximum depth of oxygen in Sample S6 is smaller than that in Sample S5. It may be attributed to different Al implantation dosages [23].

The Cu 2p XPS spectra of Samples S4, S5, and S6 are depicted in Fig. 3 and the possible Cu phases are listed in Table 2. It can be observed that copper mainly exists in the form of CuO (binding energies of 933.6 and 953.6 eV) on the surface and near the surface of Sample S4. The CuO peak is dominant up to a depth of about 26 nm and as expected, the content of CuO decreases with increasing depth in Sample S4. In contrast, elemental copper (binding energies of 932.2 and 952.0 eV) is the main form near the surface of Samples S5 and S6 except for trace Cu₂O, and almost all of copper exists

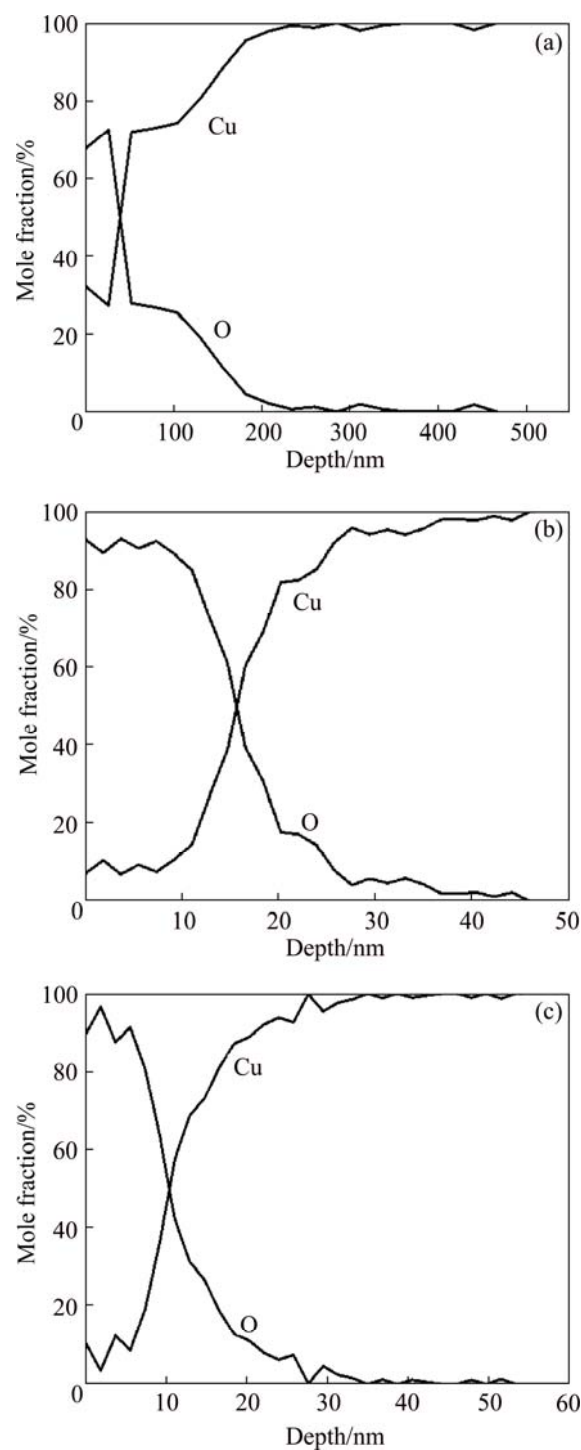


Fig. 2 Depth profiles of Cu and O in Samples S4 (a), S5 (b), and S6 (c)

in the form of elemental copper when the depth is 3.68 nm. The results indicate that copper samples are effectively protected from surface oxidation by Al implantation.

Figure 3 and Table 2 show that the Cu 2p peaks at 0 and 1.84 nm in Samples S5 and S6 are very weak and the main reason may be that the introduction of Al to the near surface region in Samples S5 and S6 lowers the relative content of copper. By comparing Samples S5 and

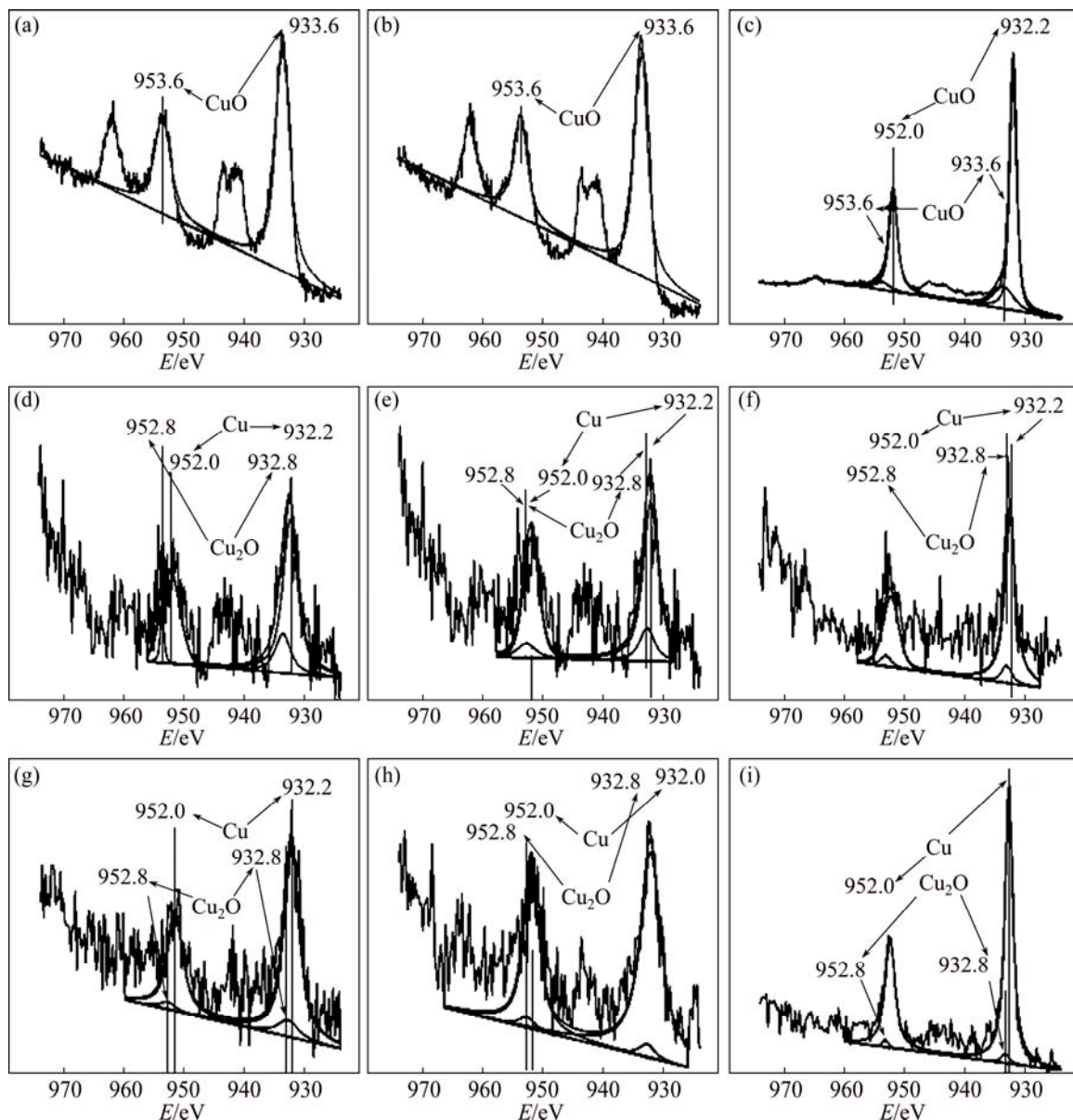


Fig. 3 Cu 2p core level binding energy spectra of Samples S4 (a, b, c), S5 (d, e, f), and S6 (g, h, i): (a, d, g) Depth of 0 nm; (b) Depth of 25.91 nm; (c) Depth of 51.82 nm; (e, h) Depth of 1.84 nm; (f, i) Depth of 3.68 nm

Table 2 Possible Cu phases in outermost and near surface of Samples S4, S5 and S6

Sample No.	Depth/nm	Existing form of copper	Peak intensity
S4	0	▲*	Strong
	25.91	▲	Strong
	51.82	▲(s)+○(s)	—
S5	0	Δ(m)+○(s)	—
	1.84	Δ(w)+○(s)	—
	3.68	Δ(w)+○(s)	—
S6	0	Δ(w)+○(s)	—
	1.84	Δ(w)+○(s)	—
	3.68	Δ(w)+○(s)	—

▲, Δ and ○ represent CuO, Cu₂O and Cu, respectively; w, m and s represent intensity degree of peak: weak, middle and strong, respectively

S6 (Fig. 3), it can be found that higher content of Cu₂O exists in the outermost layer of Sample S5 than that in the outermost layer of Sample S6. The results suggest that different Al implantation fluencies affect the oxidation resistance of copper to some degree.

3.3 Antibacterial activity

The bacteria, *Staphylococcus aureus*, are used to assess the antibacterial activity of pure copper and plasma implanted copper specimens. After culturing for 24 h, an antibacterial rate of almost 100% is observed from both the pure and implanted Cu samples subjected to 2×10^5 – 5×10^5 CFU/mL *Staphylococcus aureus*. The results acquired from Samples S1, S2 and S3 are summarized in Table 3, which illustrates that Al-PIII and

Table 3 Antibacterial activities of Samples S1, S2, S3 and control (C)

Sample No.	S1 ₁	S1 ₂	S1 ₃	S2 ₁	S2 ₂	S2 ₃	S3 ₁	S3 ₂	S3 ₃	C ₁	C ₂	C ₃
Antibacterial rate/%	100	100	100	100	100	100	100	100	100	0	0	0

S1₁, S1₂, S1₃, S2₁, S2₂, S2₃, S3₁, S3₂ and S3₃ are parallel samples of S1, S2 and S3, respectively; C₁, C₂ and C₃ are parallel samples of control C

N-PIII have no effect on the antibacterial properties of copper, especially for *staphylococcus aureus*. In comparison, the antibacterial rate observed from the negative control is 0.

The plasma treated copper samples possess both higher surface microhardness and enhanced oxidation resistance while maintaining their high antibacterial activity. Al implanted Cu offers higher oxidation resistance due to the protective Al implanted layer and it is shown in our experiments that this modified layer does not degrade the antibacterial rate.

There are two possible reasons. Firstly, copper is an excellent antibacterial agent, especially to *Staphylococcus aureus* and *Escherichia coli*. A low content copper on the surface of other materials can indeed provide high antibacterial rates against the two types of bacteria. According to the study of ZHANG et al [24], a content of about 3% copper (mass fraction) in the near surface of Cu plasma implanted polyethylene can produce an antibacterial rate of 86.1% against *Staphylococcus aureus*. As shown in Fig. 5 in Ref. [23], the content of copper in the outermost surface on the plasma implanted specimens is about 20% and the Cu content increases with the increase of the depth. Thus, there is an excess supply of Cu from the substrate during the prolonged exposure, thereby rendering the materials with excellent antibacterial properties. Secondly, the surface Al implanted layer has a thickness of about tens of nanometers. When pure Cu undergoes natural oxidation, oxygen penetrates the surface oxide readily, causing continuous oxidation. On the contrary, in the Al implanted Cu samples, most of the incoming oxygen atoms are captured by Al on the near surface due to high chemical affinity between O and Al. Oxygen is thus trapped to form aluminum oxide which impedes further diffusion of oxygen to the bulk of the materials. At the same time, copper atoms from the bulk can diffuse to the surface because the binding force between Cu and Al is much lower than that between O and Al. Consequently, there are enough copper ions on the surface of the Al plasma implanted Cu samples to provide the excellent antibacterial capability.

4 Conclusions

1) Surface hardness of copper can be enhanced by Al and N plasma immersion ion implantation, and its values will increase with larger Al implantation dosages

during a certain range. The higher surface hardness determined from the plasma treated copper samples stems from lattice distortion resulting from irradiation damage and defects such as cavities and interstitial atoms introduced by PIII.

2) Al and N plasma immersion ion implantation can improve the oxidation resistance of pure copper. The oxidation tests and XPS analysis results also show that the degree of oxidation resistance depends on the Al implantation dosages.

3) PIII-treated copper samples with different Al dosages show excellent antibacterial properties arising from the synergistic effect that copper provides a high antibacterial rate against *Staphylococcus aureus*. Simultaneously, Al atoms on the near surface of copper provide resistance to oxidation of the copper substrate.

References

- [1] CHOI W S, KIM J. Laser-assisted deposition of Cu bumps for microelectronic packaging [J]. Transactions of Nonferrous Metals Society of China, 2012, 22(S3): s683–s687.
- [2] SHARIFAHMADIAN O, SALIMIJAZI H R, FATHI M H, MOSTAGHIMI J, PERSHIN L. Relationship between surface properties and antibacterial behavior of wire arc spray copper coatings [J]. Surface & Coatings Technology, 2013, 233: 74–79.
- [3] PRAMANIK A, LAHA D, BHATTACHARYA D, PRAMANIK P, KARMAKAR P. A novel study of antibacterial activity of copper iodide nanoparticle mediated by DNA and membrane damage [J]. Colloids and Surfaces B, 2012, 96: 50–55.
- [4] BAGCHI B, KAR S, DEY S K, BHANDARY S, ROY D, MUKHOPADHYAY T K, DAS S, NANDY P. In situ synthesis and antibacterial activity of copper nanoparticle loaded natural montmorillonite clay based on contact inhibition and ion release [J]. Colloids and Surfaces B, 2013, 108: 358–365.
- [5] RAZEEB K M, PODPORSKA C J, JAMAL M, HASAN M, NOLAN M, MCCORMACK D E, QUILTY B, NEWCOMB S B, PILLAI S C. Antimicrobial properties of vertically aligned nanotubular copper [J]. Materials Letters, 2014, 128: 60–63.
- [6] ZIMMERMANN M, UDAGEDARA S R, SZE C M, RYAN T M, HOWLETT G J, XIAO Z G, WEDD A G. PcoE-A metal sponge expressed to the periplasm of copper resistance *Escherichia coli*: Implication of its function role in copper resistance [J]. Journal of Inorganic Biochemistry, 2012, 115: 186–197.
- [7] KIRAKOSYAN G, TRCHOUNIAN A. Redox sensing by *Escherichia coli*: Effects of copper ions as oxidizers on proton-coupled membrane transport [J]. Bioelectrochemistry, 2007, 70(1): 58–63.
- [8] LEKKA M, BONORA P L, LANZUTTI A, BENONI S, CAODURO P, FEDRIZZI L. Industrialization of Ni-mu SiC electrodeposition on copper moulds for steel continuous casting [J]. Metallurgia Italiana, 2012, 104(6): 21–27.
- [9] LAMOVEC J, JOVIC V, VORKAPIC M, POPOVIC B, RADOJEVIC V, ALEKSIC R. Microhardness analysis of thin

- metallic multilayer composite films on copper substrates [J]. Journal of Mining and Metallurgy Section B, 2011, 47(1): 53–61.
- [10] YANG Guang-bin, CHAI Shan-tao, XIONG Xiu-juan, ZHANG Sheng-mao, YU Lai-gui, ZHANG Ping-yu. Preparation and tribological properties of surface modified Cu nanoparticles [J]. Transactions of Nonferrous Metals Society of China, 2012, 22(2): 366–372.
- [11] KOO H C, CHO S K, KWON O J, SUH M W, IM Y, KIM J J. Improvement in the oxidation resistance of Cu films by an electroless Co-alloy capping process [J]. Journal of the Electrochemical Society, 2009, 156(7): D236–D241.
- [12] CHEN S S, BROWN L, LEVENDORF M, CAI W W, JU S Y, EDGEWORTH J, LI X S, MAGNUSON C W, VELAMAKANNI A, PINER R D, KANG J Y, PARK J, RUOFF R S. Oxidation resistance of grapheme-coated Cu and Cu/Ni alloy [J]. Acs Nano, 2011, 5(2): 1321–1327.
- [13] WANG Hong-xing, ZHANG Yan, CHENG Jia-lia, LI Yu-shan. High temperature oxidation resistance and microstructure change of aluminized coating on copper substrate [J]. Transactions of Nonferrous Metals Society of China, 2015, 25(1): 184–190.
- [14] MENG X P, WEN J Q, YAO Y D, DING Y, GONG Y C, ZOU C W, YIN G F, LIAO X M, HUANG Z B, CHEN X C. A facile synthesis of monodispersed carbon-encapsulated copper nanoparticles with excellent oxidation resistance from a refluxing-derived precursor [J]. Chemistry Letters, 2013, 42(6): 627–629.
- [15] DENG B, TAO Y, GUO D L. Effects of vanadium ion implantation on microstructure, mechanical and tribological properties of TiN coatings [J]. Applied Surface Science, 2012, 258(22): 9080–9086.
- [16] TIMMERS H, GLADKIS L G, WARNER J A, BYRNE A P, DELGROSSO M F, ARBEITMAN C R, GARCIA B G, GERUSCHKE T, VIANDEN R. Polymer tribology by combining ion implantation and radionuclide tracing [J]. Nuclear Instruments & Methods in Physics Research Section B, 2010, 268 (11–12): 2119–2123.
- [17] PEI Y L, LUAN Y. Surface modification of NiTi alloys using nitrogen doped diamond-like carbon coating fabricated by plasma immersion ion implantation and deposition [J]. Journal of Alloys and Compounds, 2013, 581: 873–876.
- [18] CHU P K. Progress in direct-current plasma immersion ion implantation and recent applications of plasma immersion ion implantation and deposition [J]. Surface & Coatings Technology, 2013, 229: 2–11.
- [19] WANG M, REN F, CAI G X, LIU Y C, SHEN S H, GUO L J. Activating ZnO nanorod photo-anodes in visible light by Cu ion implantation [J]. Nano Research, 2014, 7(3): 353–364.
- [20] POGREBNJAK A D, SHYPYLENKO A P, AMEKURA H, TAKEDA Y, OPANASYUK A S, KURBATOV D I, KOLOTOVA I A, KLYMOV O V, KOZAK C. Effect of Cu negative ion implantation on physical properties of $Zn_{1-x}Mn_xTe$ films [J]. Acta Physica Polonica A, 2013, 123(5): 939–942.
- [21] ZHANG X D, XI J F, SHEN Y Y, ZHANG L H, ZHU F, WANG Z, XUE Y H, LIU C L. Thermal evolution and optical properties of Cu nanoparticles in SiO_2 by ion implantation [J]. Optical Materials, 2011, 33(3): 570–575.
- [22] HONG J H, LEE Y, HAN S, KIM K J. Improvement of adhesion properties for Cu films on the polyimide by plasma source ion implantation [J]. Surface & Coatings Technology, 2006, 201(1–2): 197–202.
- [23] AN Q Z, LI L H, HU T, XIN Y C, FU R K, KWOK D T, CAI X, CHU P K. Comparison of oxidation resistance of copper treated by beam-line ion implantation and plasma immersion ion implantation [J]. Materials Chemistry and Physics, 2009, 116(2–3): 519–522.
- [24] ZHANG W, JI J H, ZHANG Y H, YAN Q, CHU P K. Chemical and physical properties of copper and nitrogen plasma-implanted polyethylene [J]. Plasma Processes and Polymers, 2007, 4(2): 158–164.

Al 和 N 等离子浸没注入对铜表面硬度、氧化和抗菌性能的影响

安全长^{1,2,3}, 冯凯¹, 吕和平¹, 蔡珣¹, 孙铁国³, 朱剑豪²

1. 上海交通大学 材料科学与工程学院 上海市激光制造与材料改性重点实验室, 上海 200240;

2. 香港城市大学 物理与材料科学系, 香港 999077;

3. 常州亿晶光电科技有限公司, 常州 213200

摘要: 采用等离子浸没注入方法(PIII)将 Al 和 N 注入铜基体中, 以提高铜的硬度和抗氧化性能。其中氮离子注入剂量为 $5 \times 10^{16} \text{ cm}^{-2}$, 铝离子注入剂量范围为 $5 \times 10^{16} \sim 2 \times 10^{17} \text{ cm}^{-2}$ 。氧化实验表明, 铜的抗氧化性能随铝离子注入剂量变化; 抗菌实验结果表明, 对于金黄色葡萄球菌, 等离子浸没注入的铜样品具有与纯铜同样优异的抗菌抑菌性能。

关键词: 铜; 等离子浸没注入; 纳米压入; 抗氧化; 抗菌性能

(Edited by Wei-ping CHEN)